IEEE Photonics Journal
An IEEE Photonics Society Publication

A Hybrid Optical Fiber and FSO System for Bidirectional Communications Used in Bridges

Volume 7, Number 6, December 2015

Yi-Lin Yu
Shien-Kuei Liaw
Hsi-Hsir Chou
Hoa Le-Minh
Zabih Ghassemlooy

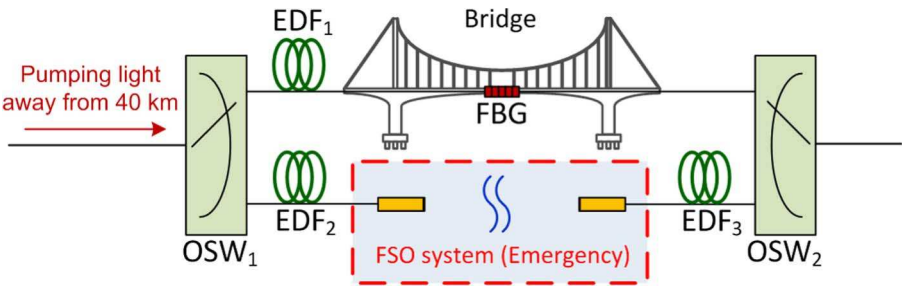

DOI: 10.1109/JPHOT.2015.2488286
1943-0655 © 2015 IEEE

A Hybrid Optical Fiber and FSO System for Bidirectional Communications Used in Bridges

Yi-Lin Yu,[1] Shien-Kuei Liaw,[1] Hsi-Hsir Chou,[1] Hoa Le-Minh,[2] and Zabih Ghassemlooy[2]

[1]Department of Electronic and Computer Engineering, National Taiwan University of Science and Technology, Taipei 106, Taiwan.
[2]Faculty of Engineering and Environment, Northumbria University Newcastle upon Tyne, NE1 8ST, U.K.

DOI: 10.1109/JPHOT.2015.2488286

Manuscript received October 2, 2015; accepted October 2, 2015. Date of publication October 7, 2015; date of current version December 7, 2015. This work was supported in part by MOST of Taiwan under Grant 103-2221-E-011-021. Corresponding author: Y.-L. Yu (e-mail: d9802301@yahoo.com.tw).

Abstract: In this paper, a 10-Gb/s hybrid optical fiber (OF) and free-space optics (FSO) link as part of a bidirectional long-haul OF transmission for application in outdoor environments such as bridges is proposed. A fiber-Bragg-grating (FBG) sensor head is used for monitoring the condition of a bridge, and in the case of the bridge being damaged, the transmission path is changed over from OF to the FSO link to ensure link connectivity. An Erbium-doped fiber amplifier is used to compensate for losses due to the fiber cable and the free-space channel. At a bit error rate (BER) of 10e-9, the power penalty between the OF and FSO paths is < 1 dB, and the power variations for both paths are ±0.07 and ±0.12 dB, respectively.

Index Terms: Free space optics, erbium doped fiber amplifier, fiber sensor, long-haul transmission system.

1. Introduction

Free space optics (FSO) systems have become an important research topic in recent years thanks to its infrastructure flexibility whilst offering license free, and cost effective, very-high-speed communications. FSO could simply be setup as a point-to-point transmission link in outdoor environment [1], [2] as a backup in situation where the cable based telecommunications infrastructures are severely damaged due to natural and human made disasters. Thus, offering a viable high-speed communications facility for the medical and emergency services as well as the media reporters. Most research work reported so far and commercial systems available are based on the FSO or hybrid FSO radio-frequency-based technologies with a few on the hybrid optical fiber and FSO (HOF-FSO) schemes [3]–[6]. In [7], an experimental work on a 2 × 80 Gbps dense wavelength division multiplexing (DWDM) based bidirectional wavelength reuse optical wireless transmission is reported. In [8], a FSO system with coupling single-mode fiber (SMF) optical fiber (OF) was reported, where collimators with a symmetrical configuration was used for focusing the light between the links two SMFs. However, no data was given on the performance of the proposed system. An ultra-high capacity system based on a passive optical network (PON) and a FSO link was reported in [9]. In this work, the FSO link is only utilized at the optical network

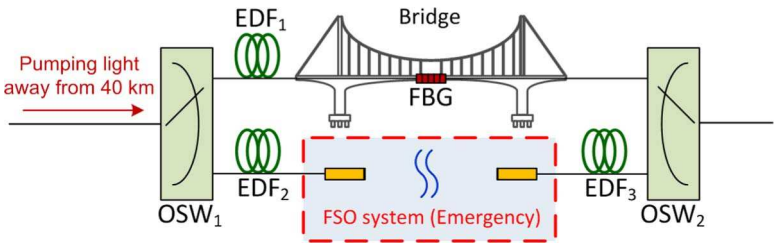

Fig. 1. Proposed hybrid HOF-FSO system.

unit (ONU) of the PON. In this paper, we propose and demonstrate a bidirectional cross-bridge communications system, which includes the FSO link that could be used as a long-haul transmission backup link in emergency situations. In this system the FSO link is established across a bridge to provide emergency communications backup to the OF link, which could be damaged due to natural/artificial disasters. In additional, in FSO based link air humidity (or fine water particles in the form of fog) will result in signal attenuation. Since the transmission distance is too short, then the effect of fog (water droplet) induced attenuation is not that significant to effect the link availability [10]. A fiber Bragg grating (FBG)-based sensor is incorporated into the SMF for monitoring forces experienced by the bridge. On detecting unusual behaviors on the bridge due to external forces or in the case of the bridge structurally being damaged the transmission mode is promptly switched over from OF to the FSO link. In addition, we have used a pump sharing Erbium-doped fiber amplifier (EDFA) in both links to compensate for losses due to OF, optical components, and the FSO channel. We have developed a testbed to verify the system operation and evaluate its performance in terms of the link bit error rate (BER), eye-diagram and optical signal-to-noise ratio (OSNR).

The paper is organized as followed: Section 2 will present the proposed system and the experiment setup. The results and discussions will be given in Section 3, and the paper will be concluded in Section 4.

2. Experimental Setup

The proposed system made up of HOF and FSO links is depicted in Fig. 1, which is composed of a wavelength selective coupler (WSC), an 1×2 optical switch pairs (OSWs), and a FBG. The 1×2 optical switch (Chin Optics cooperation, Model No YM141NL) has an insertion loss, a polarization dependent loss and a switching speed of 0.7 dB, 0.05 dB and 3.5 ms, respectively. In a 10 Gb/s modulated speed, the data loss for our 1×2 optical switch are $10^{10} \times 3.5 \times 10^{-3} = 3.5 \times 10^{7}$ during port switching. Nevertheless, the proposal in this work is focused on emergency situation, so the data loss and system downgrade within duration of mini seconds are acceptable. To reduce the data loss, an electro-optical switch with a faster switching time down to sub-nanosecond [11] could be used instead. It is used to switch over between the OF and FSO paths. The absorption coefficient and the length of $EDFA_1$ are 5 dB/m@979 nm and 5 m, respectively. Whereas, the absorption coefficient and the lengths for $EDFA_{2\&3}$ are 12.4 dB/m@979 nm, 2 m and 1 m, respectively. Using a combination of EDFAs, the minimum variation in power between the OF and FSO paths can be readily achieved. The pump laser diode (LD) was set at the central office, and the residual pump power was at 42 mW when switching to the upper (OF) or bottom (FSO) path. For the upper path, $EDFA_1$ not only acts as the gain medium, but it is also used as a light source for the FBG based sensor. The fabricated FBG with a large reflectivity of 99.7% is used to monitor the physical conditions of the bridge, and on detecting any problems the signal transmission path is changed over from OF to FSO. The FSO link is composed of two transceiver terminals (TT) with customized single mode (SM) collimators used for accurate alignment between the TT. A 10X objective lens and a convex lens with a diameter of 24 mm and a focal length of 13 cm are used to optimize the optical beam size and the power loss. Both the transmitter and receiver terminals in the original experimental setup were based on SM collimators to

TABLE 1

System parameters

Pump power	440 mW	Pumping wavelength	1480 nm
EDF_1 (coefficient and length)	5dB/m@979nm and 5 m	FSO system (distance)	10 m
EDF_2 (coefficient and length)	12.4dB/m@979nm and 2 m	FSO system (loss)	4.23
EDF_3 (coefficient and length)	12.4 dB/m@979nm and 1 m	FBG (wavelength)	1538.25
10X objective lens (diameter)	24 mm	FBG (reflectivity)	99.70%
Convex lens (focal length)	13 cm		

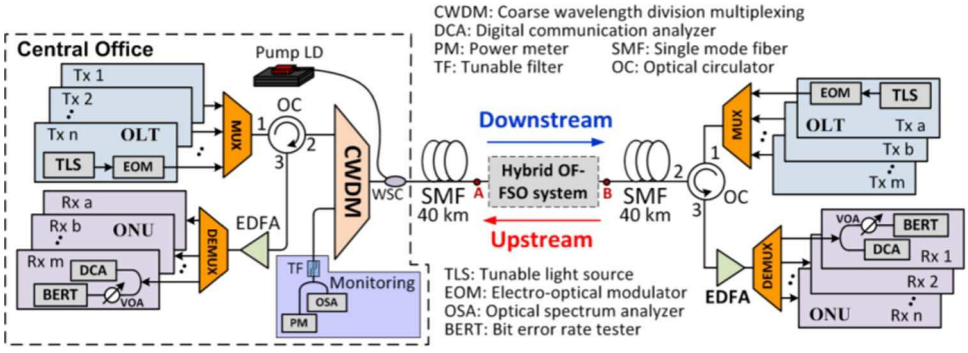

Fig. 2. Long-haul transmission scheme with the hybrid HOF-FSO system.

ensure low chromatic dispersion at a data rate of < 10 Gb/s. On the other hand, using the multimode (MM) collimator with a large core area together with the MM fiber makes helps signal alignment in the FSO system but at the cost of degradation of the system performance due to the chromatic dispersion in both the MM collimator and MM fiber. All the key parameters for the proposed system are shown in Table 1.

Fig. 2 shows a schematic diagram of the bidirectional long-haul OF transmission system including the proposed HOF-FSO system. Such a system could be used to connect to a number of parallel HOF-FSO links. The pump LD source is located within the central office between the CWDM and a 40-km SMF spool. In such case, the pump LD acts as a remote pump for the hybrid HOF-FSO system. Using higher pump power of 440 mW to compensate for the fiber loss of 0.22 dB/km @1480 nm, we observed no changes in the BER performance based on the location of the pump LD. In Fig. 2 each optical line terminal (OLT) contains four transmitters, four receivers, two array waveguide gratings (AWGs), an optical circulator (OC), and an EDFA. In addition, OLT on the left is composed of a coarse wavelength division multiplexing (CWDM), a tunable filter (TF), a power meter (PM) and an optical spectrum analyzer (OSA). CWDM is used to direct the reflected light from FBG within the HOF-FSO path to the monitoring unit.

In our previous work [7], we reported that the FSO transmission distance can be extended by simply adjusting the position and parameter of the convex lens at terminals A and B, respectively. In this work, we have used a SM collimator as the transceiver terminal. The SM collimator can be readily connected to the OF cable. However, the small core area of the SMF will limit the FSO transmission span to only 40 m, which is long enough for installation in bridges. Fig. 3 illustrates the concept of laser beam transmission when employing convex lenses with SM and MM collimators. For a Gaussian beam propagating through the in free space channel, the spot size $W(z)$ will be a minimum value W_0 at one position along the z-axis, which is known as the beam waist. The relationship between the spot size and the distance z is given by

$$W(z) = W_0\sqrt{1+\left(\frac{z}{z_0}\right)^2}; \quad z_0 = \frac{\pi W_0^2}{\lambda} \tag{1}$$

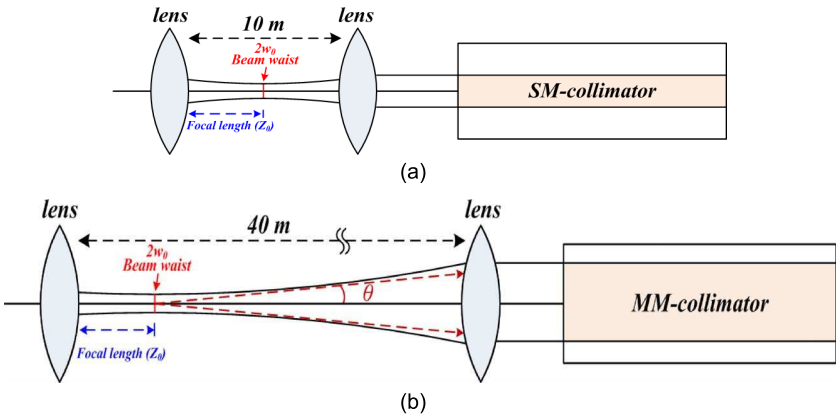

Fig. 3. Depth of focus Gaussian beam for receiving by (a) a SM-collimator and (b) a MM-collimator.

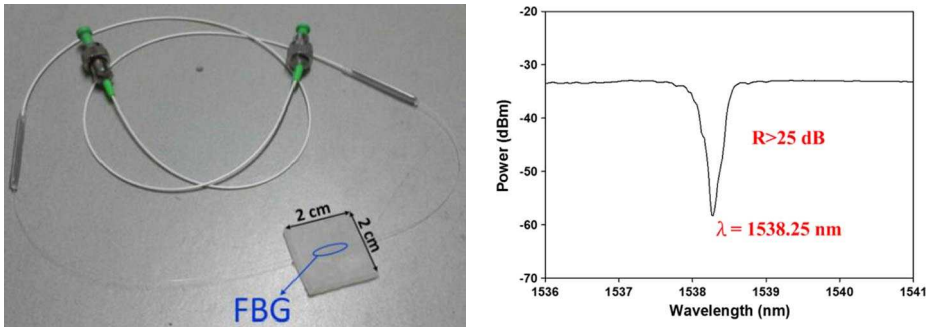

Fig. 4. (a) FBG fiber sensor head and (b) the measured transmission spectrum of FBG.

where z_0 is the focal length [12]. Equation (1) shows that the transmission distance is proportional to the square of $W(z)$. Therefore, in order to extend the transmission distance, a MM collimator could be used as the receiving terminal since the OF core area is an order larger than that of a the SM collimator. Note that the length of the MM connected to MM collimator needs to be kept short to avoid large fiber induced chromatic dispersion.

2.1 FBG Sensor

FBG can be used for sensing, such as strain, temperature, and refractive index, etc. [13], [14]. Fig. 4(a) show a FBG used as the sensing head for the proposed system. The Bragg wavelength for this FBG is given by [15]

$$\lambda_B = n_{eff}\Lambda \tag{2}$$

where Λ is the period of grating and n_{eff} is the effective index of the OF, which can be altered by means of applying a force ΔP and/or changing the temperature ΔT. The relationship between the wavelength shift $\Delta\lambda$, ΔP, and ΔT are given by [15]

$$\frac{\Delta\lambda}{\lambda} = \frac{\Delta(n_{eff}\Lambda)}{n_{eff}\Lambda} = \left[\frac{1}{\Lambda}\frac{\partial\Lambda}{\partial P} + \frac{1}{n_{eff}}\frac{\partial n_{eff}}{\partial T}\right]\Delta P + \left[\frac{1}{\Lambda}\frac{\partial\Lambda}{\partial P} + \frac{1}{n_{eff}}\frac{\partial n_{eff}}{\partial T}\right]\Delta T \tag{3}$$

where Δn_{eff} and $\Delta\Lambda$ are the variation of effective index and the period of FBG, respectively. In this work, the FBG is coated with a layer of silicon as shown in Fig. 4(a). It can increase both the sensing area and the applied force. The device fabricated was thick, and therefore, both ΔP

and ΔT of the FBG were determined by the clastic and thermal properties of the silicon. Therefore, eq. (3) can be simplified as [16]

$$\frac{\Delta\lambda}{\lambda} = -k_{\varepsilon}(1-2\upsilon)\frac{\Delta P}{E} + (k_{\varepsilon}\alpha + k_T)\Delta T \tag{4}$$

where υ and E are the Poisson ratio and Young modulus of the silicon, respectively. α is the thermal expansion coefficient of the silicon, k_{ε} and k_T are the constants that depends on the photo-elastic coefficient and thermal expansion coefficient of the OF, respectively. Assuming the room temperature the second term of (4) could be neglected. Therefore, the wavelength shift induced by ΔP is given as

$$\frac{\Delta\lambda}{\lambda} = -k_{\varepsilon}(1-2\upsilon)\frac{\Delta P}{E} \tag{5}$$

Obviously, $\Delta\lambda$ has a linear relationship with ΔP.

3. Results and Discussion

First, we assessed the characteristics and performance of the FBG based sensor that was positioned along the bridge. The reflected signal from the FBG is transmitted to the OLT unit for monitoring the condition of the bridge. Fig. 4(b) shows the measured transmission spectrum of the high reflectivity FBG (> 25 dB), which were used in the system.

The measured reflected lights from the FBG and the passband of TF are shown in Fig. 5(a). Note that the wavelength of reflected light is shifted to longer wavelength with ΔP. Therefore the measured output power is decreased due to the insertion loss of TF. In Fig. 5(b), the black-solid and blue-dash curves are the measured output power and peak power, respectively. The peak power is defined as the peak of FBG reflected spectrum measured by an OSA; the total power including signal power and noise are measured using an optical power meter. Because the 3 dB bandwidth of TF is larger than the reflected light from FBG, the measured output power is higher than peak power. To verify the theoretical result, we also measured the relationship between $\Delta\lambda$ and ΔP, showing a linear profile as shown in Fig. 4(b), thus confirming the predicted data.

To verify overall system operation and evaluate its performance, we used a multi-channel laser array in the C band with wavelengths of 1545.50-, 1549.14-, 1552.38-, and 1555.48-nm for the downstream transmission, and 1547.35-, 1551.03-, 1554.07-, and 1557.05-nm for the upstream transmission. The launch power per channel was set at around –4 dBm. The measured power spectrums observed at the OLT and at output of the OF path after passing through a 40 km of SMF are shown in Figs. 6 and 7, respectively. For the OF path, see Fig. 7, the output power of each channel is about 6 dBm, the power level variation between channels is <1 dB, the average power is –6.22 dBm, and the dynamic range is ~39 dB.

For the case of FSO path, the output power spectra of both the downstream and upstream transmissions are depicted in Fig. 8. The output power of each channel and the power level variation among channels are –6 dBm and ~1 dB, respectively, as in Fig. 6. The average power is –5.68 dBm, which is marginally lower than –6.22 dBm as in Fig. 7. Note the power dynamic range for the downstream is the same as in Fig. 7, whereas for the upstream, it is lower by ~2 dB. This is due to the higher noise level as result of backward pumping and using a two-stage EDFA. In order to verify the stability of the proposed system, we monitored and measured the power variation between the OF and FSO paths (see Fig. 2) for a duration of 20 minutes, and the results are illustrated in Fig. 9(a) and (b) for both OF and FSO paths, respectively. Note that the power variations are ±0.07 dB and ±0.12 dB for the OF and FSO paths, respectively. The reason for higher value of power variation for the FSO path is because of sensitivity of the FSO link to the vibration, expansion, and contraction of a bridge.

To investigate the proposed HOF-FSO system for deployment across the bridge as shown in Fig. 2, one channel at a wavelength of 1549.4 nm was externally modulated using a 10 Gb/s

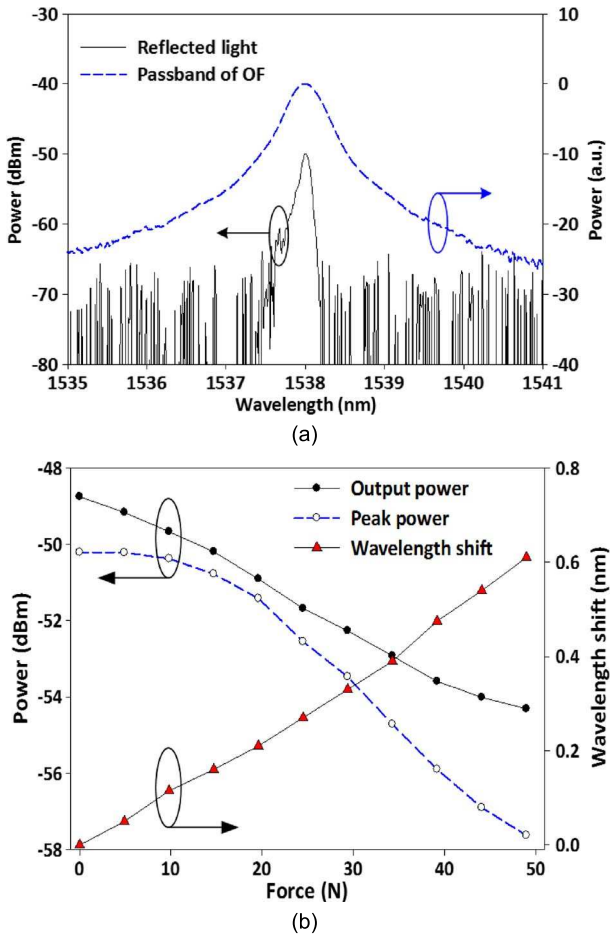

Fig. 5. (a) Measured passband of TF and reflected light from the FBG of the sub-system and (b) measured received power and wavelength shift with difference applied force.

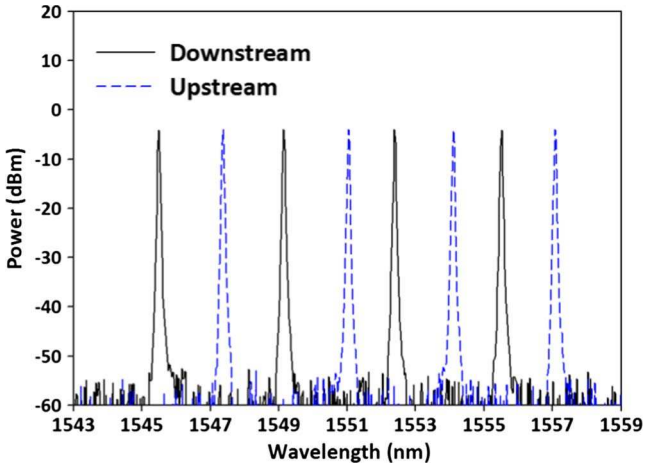

Fig. 6. Power spectrums at the output of the optical line terminal.

electro-optic modulator (EOM). We used a pseudo random bit sequence (PRBS) of length $2^{31} - 1$ in the non-return-to-zero (NRZ) signal format. Fig. 10 shows the measured BER performance for the 80 km transmission for both OF and FSO paths. At a BER of 10e-9, the power penalty

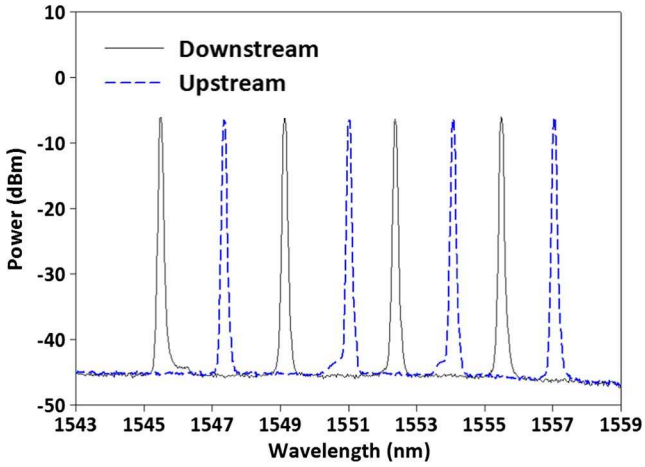

Fig. 7. Measured output spectra of channels which propagate via the OF path at point "B" (downstream) and point "A" (upstream), respectively. All channels were amplified by the EDFA inside this HOF-FSO system.

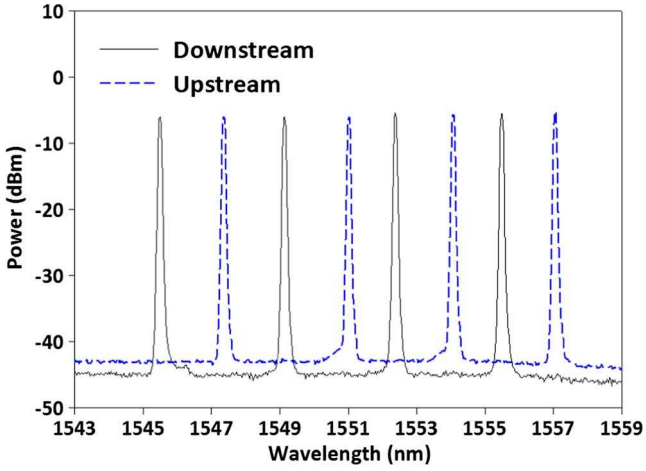

Fig. 8. Measured output spectra of channels which propagate via the FSO path at point "B" (downstream) and point "A" (upstream), respectively. All channels were amplified by the EDFA inside this HOF-FSO system.

between the OF and FSO paths is 0.73 dB, which is rather low. However, with more pump power available, the power penalties can be readily decreased by simply increasing the signal to noise ratio. Finally we measured the eye-diagrams of the OF and FSO paths using a digital communication analyzer (DCA), as depicted in Fig. 11(a) and (b), respectively, thus demonstrating high quality signal transmission across both paths.

4. Conclusion

We have proposed and investigated a bidirectional long-haul optical fiber transmission, which included a hybrid OF-FSO system for emergency communications deployed across a bridge. The reflected signal from the FBG based sensor positioned along bridge was used to monitor the condition of the bridge. The relationship between wavelength shift and applied force of FBG was measured experimentally, which was used to predict the abnormal condition of the bridge, thus enabling the switching from OF transmission mode to FSO system. Signals attenuation mainly due to the SMF, the FSO channel and fiber components were compensated using a number of

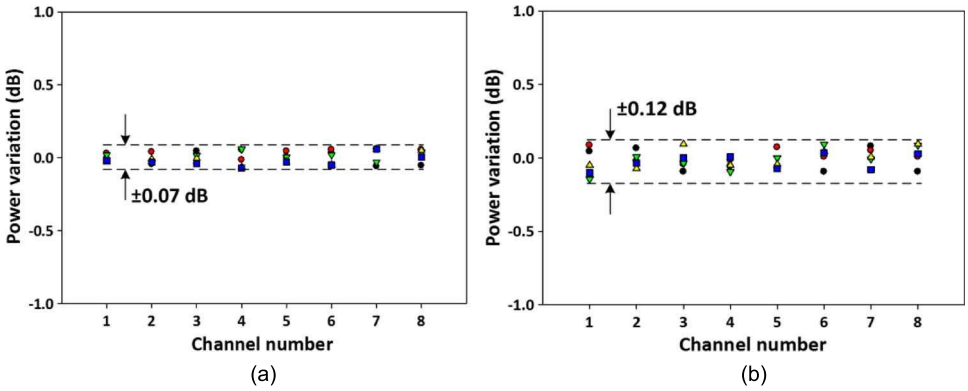

Fig. 9. Measured power variations. (a) OF path. (b) FSO paths with 40 km of SMF.

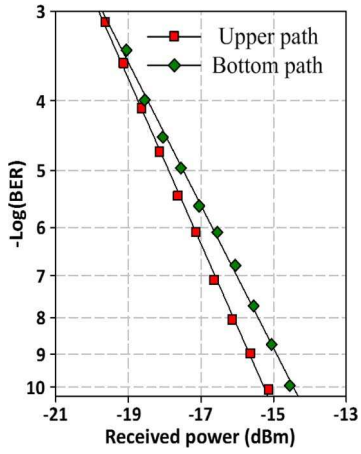

Fig. 10. Measured BER performance of the proposed system at 1549.4 nm for the upper path (OF) and bottom path (FSO), respectively.

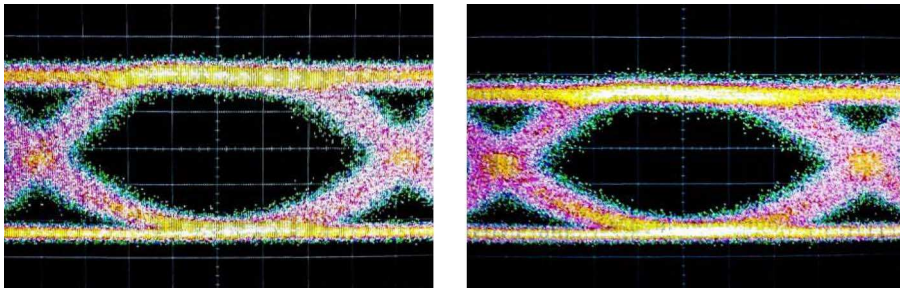

Fig. 11. Measured the eye diagrams for signal propagation through 80 km of SMF and via (a) the upper (OF) and (b) the bottom (FSO) paths, respectively.

EDFAs. The output power levels between the optical fiber and FSO paths were less than 1 dB, whereas the power variation for both paths were ±0.07 dB and ±0.12 dB, respectively. For both OF and FSO paths the measured BER performance confirmed low error rates (i.e., 10e-3) with a very low power penalty of 0.73 dB between the OF and FSO paths for the 80-km transmission under test. In addition, the measured eye-diagrams also showed an acceptable performance

over a long transmission range for the OF and FSO paths. With more pump power available and dispersion compensation schemes the system transmission span can be extended to 100 km. Though the paper has demonstrated a link with a bridge, in general, it is possible to have more bridges or infrastructures that require hybrid OF-FSO links to ensure seamless communications.

Acknowledgment

K. Y. Hsu's and Y. C. Chou's help are much appreciated.

References

[1] P. J. Winzer and R. J. Essiambre, "Advanced modulation formats for high-capacity optical transport networks," *J. Lightw. Technol.*, vol. 24, no. 12, pp. 4711–4728, Dec. 2006.
[2] A. H. Gnauck, R. W. Tkach, A. R. Chraplyvy, and T. Li, "High-capacity optical transmission systems," *J. Lightw. Technol.*, vol. 26, no. 9, pp. 1032–1045, May 2008.
[3] T. Tsujimura, K. Yoshida, T. Kurashima, and M. Mikawa, "Trans-window free space optics transmission system," in *Proc. SICE Annu. Conf.*, 2008, pp. 79–82.
[4] E. Ciaramella *et al.*, "1.28-Tb/s (32 $\times$ 40 Gb/s) free-space optical WDM transmission system," *IEEE Photon. Technol. Lett.*, vol. 21, no. 16, pp. 1121–1123, Aug. 2009.
[5] R. Paudel, Z. Ghassemlooy, H. Le-Minh, and S. Rajbhandari, "Modelling of free space optical link for ground-to-train communications using a Gaussian source," *IET Optoelectron.*, vol. 7, no. 1, pp. 1–8, Feb. 2013.
[6] M. Ijaz *et al.*, "Modeling of fog and smoke attenuation in free space optical communications link under controlled laboratory conditions," *J. Lightw. Technol.*, vol. 31, no. 11, pp. 1720–1726, Jun. 2013.
[7] H. Y. Hsu *et al.*, "2 $\times$ 80 Gbit/s dense wavelength division multiplexing (DWDM) bidirectional wavelength reuse optical wireless transmission," *IEEE Photon. J.*, vol. 5, no. 4, Aug. 2013, Art. ID 7901708.
[8] K. Yoshida, K. Tanaka, T. Tsujimura, and Y. Azuma, "Assisted focus adjustment for free space optics system coupling single-mode optical fiber," *IEEE Trans. Ind. Electron.*, vol. 60, no. 11, pp. 5306–5314, Nov. 2013.
[9] A. Shahparia *et al.*, "Ultra-high-capacity passive optical network systems with free-space optical communications," *Fiber Integr. Opt.*, vol. 33, no. 3, pp. 149–162, Jul. 2014.
[10] Z. Ghassemlooy, W. O. Popoola, and S. Rajbhandari, *Optical Wireless Communications-System and Channel Modelling With Matlab*. Boca Raton, FL, USA: CRC, Aug. 2008.
[11] R. Ramaswami, K. N. Sivarajan, and G. Sasaki, *Optical Networks: A Practical Perspective*, 3rd ed. San Francisco, CA, USA: Morgan Kaufman, 2010.
[12] H. J. Sheng, W. F. Liu, K. R. Lin, S. S. Bor, and M. Y. Fu, "High-sensitivity temperature-independent differential pressure sensor using fiber Bragg grating," *Opt. Exp.*, vol. 16, no. 20, pp. 16013–16018, Sep. 2008.
[13] C. Gouveia, P. A. S. Jorge, J. M. Baptista, and O. Frazao, "Fabry–Pérot cavity based on a high-birefringent fiber Bragg grating for refractive index and temperature measurement," *IEEE Sens. J.*, vol. 12, no. 1, pp. 17–21, Jan. 2012.
[14] B. E. A. Saleh and M. C. Teich, *Fundamentals of Photonics*, 2nd ed. Hoboken, NJ, USA: Wiley-Interscience, 2007.
[15] K. O. Hill and G. Meltz, "Fiber Bragg grating technology fundamentals and overview," *J. Lightw. Technol.*, vol. 15, no. 8, pp. 1263–1276, Aug. 1997.
[16] L. Liu, H. Zhang, Q. Zhao, Y. Liu, and F. Li, "Temperature-independent FBG pressure sensor with high sensitivity," *Opt. Fiber Technol.*, vol. 13, no. 1, pp. 78–80, Sep. 2006.